

Customizing Graph Neural Networks using Path Reweighting

Jianpeng Chen^{a,b,1}, Yujing Wang^{c,1}, Ming Zeng^{d,1}, Zongyi Xiang^a, Bitan Hou^e, Yunhai Tong^c, Ole Mengshoel^g and Yazhou Ren^{a,f,*}

^aSchool of Computer Science and Engineering, University of Electronic Science and Technology of China

^bDepartment of Computer Science, Virginia Tech

^cKey Laboratory of Machine Perception, MOE, School of EECS, Peking University

^dElectrical and Computer Engineering, Carnegie Mellon University

^eShanghai Jiao Tong University

^fShenzhen Institute for Advanced Study, University of Electronic Science and Technology of China

^gDepartment of Computer Science, Norwegian University of Science and Technology

ARTICLE INFO

Keywords:

Graph neural network
Customized graph embedding
Path reweighting
Graph attention

ABSTRACT

Graph Neural Networks (GNNs) have been extensively used for mining graph-structured data with impressive performance. However, because these traditional GNNs do not distinguish among various downstream tasks, embeddings embedded by them are not always effective. Intuitively, paths in a graph imply different semantics for different downstream tasks. Inspired by this, we design a novel GNN solution, namely Customized Graph Neural Network with Path Reweighting (CustomGNN for short). Specifically, the proposed CustomGNN can automatically learn the high-level semantics for specific downstream tasks to highlight semantically relevant paths as well to filter out task-irrelevant noises in a graph. Furthermore, we empirically analyze the semantics learned by CustomGNN and demonstrate its ability to avoid the three inherent problems in traditional GNNs, i.e., over-smoothing, poor robustness, and overfitting. In experiments with the node classification task, CustomGNN achieves state-of-the-art accuracies on three standard graph datasets and four large graph datasets. The source code of the proposed CustomGNN is available at <https://github.com/cjpcool/CustomGNN>.

1. Introduction

Graph-structured datasets are receiving increasing attention since they reflect real-world data such as biological networks, social networks, citation networks, and World Wide Web. The wide range of applications demonstrates the value of mining graph structures in addressing a multitude of practical issues. Many works focus on semi-supervised learning with graph data [7, 10, 23, 42, 44]; they model the non-Euclidean space of a graph and learn structural information. Among these works, the most notable branch of studies is graph neural networks (GNNs), which embed graph-structured data through feature propagation [5, 6, 13, 20, 23, 26, 37, 41]. Intuitively, given a graph, different applications require different path weighting strategies to emphasize task-related paths and de-emphasize irrelevant ones. As shown in Figure 1(a), if we aim to optimize a node classification model by exploiting a paper citation graph, the paths between nodes from intra-class should be emphasized and the paths between nodes from inter-class should be de-emphasized. Concretely, given a citation graph where the relevance among categories is captured by path weight, if the downstream task involves classifying all papers, greater emphasis will be placed on paths that contain more nodes in the same category. If the downstream task is to find papers in a specific category (e.g., AI category), then, only the paths containing more nodes relevant to this category (AI) will be selected. Indeed, this motivation is experimentally demonstrated by our analysis (see Sections 4.5.1 and 4.5.2). Another example is about medical Q&A system on knowledge graph (shown in Figure 1(b)): If we tend to enhance the performance of medical Q&A by exploiting Wikipedia knowledge graph, some general knowledge that is not related to the medical domain (e.g., mathematical knowledge) should be de-emphasized.

*Corresponding author.

✉ jianpengc@vt.edu (J. Chen); yujwang@pku.edu.cn (Y. Wang); ming.zeng@sv.cmu.edu (M. Zeng); xzongyi@foxmail.com (Z. Xiang); houbitan@sjtu.edu.cn (B. Hou); yhtong@pku.edu.cn (Y. Tong); ole.j.mengshoel@ntnu.no (O. Mengshoel); yazhou.ren@uestc.edu.cn (Y. Ren)

ORCID(s): 0000-0001-7599-9961 (J. Chen)

¹Equal contribution.

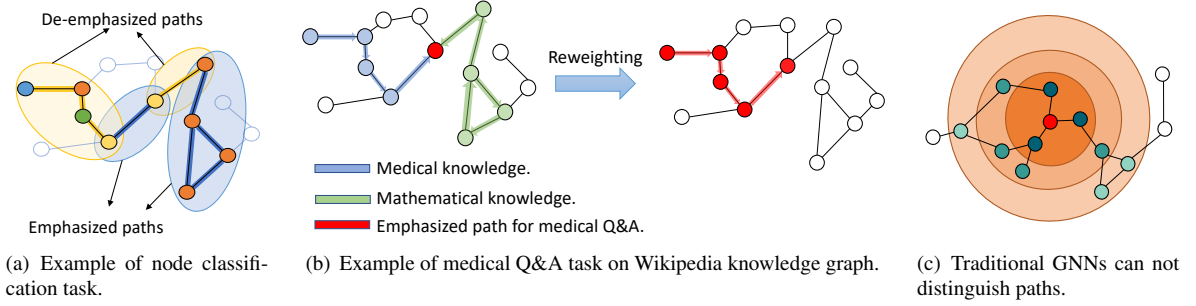


Figure 1: Examples to illustrate the intuition of path re-weighting. (a) For node classification, the paths with intra-class nodes should be emphasized (blue paths) while paths with inter-class nodes (orange paths) should be de-emphasized. (b) For medical Q&A task, each path is a piece of knowledge. Only the Q&A task-relevant paths should be emphasized. (c) Traditional GNNs aggregate neighbors order by order, neglecting the difference between paths.

However, traditional GNNs ignore the differences among paths as shown in Figure 1(c), which leads to three potential problems. 1) *Over-smoothing*: Gilmer et al. [11] states that GNNs can be regarded as a message-passing method with a low-passing filter, resulting in exponentially information lost with the increment of propagation steps, i.e., the problem of over-smoothing [29, 31]. Although some current GNNs, such as GRAND [8], GraphMix [39] and S²GNN [49], have considered multi-hop information, they are still based on the theory of message passing and ignore the differences among different paths, which also leads to the injection of task-irrelevant information and the loss of important information in the message-passing process. According to these works, the differentiation of different paths with varying hops through the message-passing method appears to be challenging. However, if we consider it from a different perspective, by extracting the high-level semantics of various paths and directly aggregating the high-order information instead of passing messages hop by hop, we can prevent information loss and noise injection while distinguishing between different paths. 2) *Poor robustness*: On the other hand, the poor robustness to graph attack [40, 48, 50] of traditional GNNs also comes from that they cannot filter out irrelevant paths and noises (e.g., the paths containing various categories in Figure 1(a) and the paths unrelated to medical knowledges in Figure 1(b)). Essentially, the propagation step aggregates all neighborhoods' information with noises, while some noisy nodes and edges may dominate the representation learning procedure. Fortunately, this issue has the chance to be addressed by de-emphasizing the paths containing these noisy nodes and edges. 3) *Overfitting*: The third issue arising from semi-supervised learning is that traditional training processes for GNNs can easily overfit the limited labeled data [30]. To address this problem, we propose a multi-perspective regularization approach and introduce a novel triplet loss, which not only enhances semantic understanding but also mitigates the risk of overfitting.

Considering these aspects, we propose Customized Graph Neural Network with Path Reweighting (CustomGNN). CustomGNN differentiates paths by extracting their high-level semantics and customizes node (graph) embeddings by aggregating high-order information directly for specific downstream tasks. In detail, CustomGNN first generates multi-perspective subgraphs. Then, a neural network with LSTM-based [19] path weighting strategy is proposed, which calculates multiple path attention maps by extracting specific high-level semantic information from these subgraphs. After that, CustomGNN aggregates features through these path attention maps so as to derive the task-oriented embeddings. Finally, we fuse these task-oriented embeddings with the generic embeddings from our multi-hop GNN. Consequently, CustomGNN can automatically filter out noise and encode the most useful structural information for specific tasks.

Furthermore, we analyze the semantics of path weights for the node classification task, which demonstrates the intuition that CustomGNN can emphasize the task-related paths while de-emphasize the irrelevant ones. We also empirically prove that our method can effectively avoid the issues of over-smoothing and non-robustness, while mitigating the issue of overfitting. Moreover, we show that the novel components proposed in this paper bring significant improvement in ablation experiments. Our contributions are concluded as follows.

- We experimentally analyzed the relevance between path weights and semantics, based on which a novel GNN architecture is proposed, named CustomGNN. CustomGNN extracts task-oriented semantic features from re-weighted paths in subgraphs and infuses the extracted information with a standard multi-hop GNN. With this

design, the proposed design of CustomGNN enables automatic noise filtering and encoding of the most relevant path structural information tailored to a specific task.

- We propose two unsupervised loss functions to regularize the learning procedure of CustomGNN. The first regularization involves utilizing random walk to generate multi-perspective subgraphs and incorporating consistency loss in-between. In the second regularization term, unlabeled data is utilized to produce pseudo-labels for enhancing semantics, followed by the application of triplet loss based on these pseudo-labels. This semantic-based design provides a new solution to adopt triplet loss with pseudo-labels for graph learning.
- As demonstrated by comprehensive experiments and analyses, the proposed CustomGNN model achieves state-of-the-art (SOTA) results on seven widely-used graph node classification datasets. It also shows high interpretability and effectively mitigates the issues of over-smoothing, non-robustness, and overfitting.

2. Related Work

2.1. Graph Neural Networks

The aim of GNNs is to learn the information structured in a graph. They achieve this by aggregating the information from neighboring nodes and learning a vector representation for each node. The core difference among different GNNs lies in their method of message passing (aggregation) [11]. For example, to aggregate information, GCN [23] proposed a graph convolution layer. GAT [37] presented graph attention layer, utilizing the feature similarity among nodes. Following GAT, Geng et al. [10] introduced graph correlated attention recurrent neural network for the task of multivariate time series forecasting. He et al. [18] proposed graph selective attention networks (SAT) to filter out irrelevant neighbors when computing attention. In contrast to GAT, Zhang et al. [46] and He et al. [17] further discussed the significance of structural information when computing attention. Specifically, Zhang et al. [46] proposed adaptive structural fingerprint (ADSF) which perceives structures by Gaussian decay and nonparametric decay; He et al. [17] introduced graph conjoint attention networks (CATs) where the structural information is fused by a proposed structural intervention generation module. However, the aforementioned two attention-based methods only attempt to perceive structural and feature information, which can be considered a subset of what CustomGNN attempts to perceive. On top of structures and features, CustomGNN, more importantly, can effectively perceive more fine-grained information, i.e., paths, and CustomGNN tends to extract high-level semantics of paths that are magnitude for different tasks. On the other hand, recently, lots of work focused on resolving the issue of over-smoothing for deep GNNs [6, 16, 26, 41, 49]. CustomGNN provides a novel view to learn graph-structured data, which focuses on learning the high-level semantics of paths for specific downstream applications. This approach naturally addresses the aforementioned issues associated with traditional GNNs.

2.2. Graph Representation Learning

Given a graph, node representation aims to learn the low-dimensional vector representation of each node and its graph-structured information. There have emerged many methods for node embedding in recent years. These methods can mainly be divided into two categories according to the input graph. The first category is sampling-based methods which use some sampling strategies, e.g., random walk [12, 44], to sample subgraphs as the input data [3, 13]. The advantage of these sampling-based methods is that they learn the local information of a graph, which can improve the model's generalization and reduce space consumption. The second category is inputting the whole graph [23, 37], and conducting specific GNNs on it to learn the node attributes and graph structure jointly. In addition, some advanced methods have emerged recently, for example, Xu et al. [42] disentangles the single representation of node attributes and graph structure into two different representations respectively. In this paper, we leverage the advantages of the sampling-based method to learn customized high-level semantic information, as well as the benefits of traditional GNNs to learn the generic graph information.

2.3. Semi-Supervised Learning on Graph

One research direction for semi-supervised learning on graphs is to assign pseudo-labels to unlabeled data. For instance, in order to utilize the unlabeled data, Lee [25] first used a neural network to infer pseudo-labels of unlabeled data. Yang et al. [43] and Hao et al. [14] performed the label propagation and pseudo-labels in the field of GNN. Schroff et al. [34] used triplet loss to enhance the uniqueness of different faces for face recognition. Similarly, for semi-supervised learning, CustomGNN combined the pseudo-labels with triplet loss to enhance the semantics of each

Table 1
The definitions of notations.

Notation	Definition
\mathbf{A}	The adjacent matrix of the given graph G .
\mathbf{F}	The attributed features of the given graph G .
$\tilde{\mathbf{F}}$	The output features from feature encoder $f_{enc}(\cdot)$ (Section 3.1).
$\hat{\mathbf{F}}$	The task-oriented features from semantic aggregation (Section 3.3).
$\dot{\mathbf{F}}$	The generic features from multi-hop GNN module.
$\overline{\mathbf{F}}^{(s)}$	$\overline{\mathbf{F}}^{(s)} = \dot{\mathbf{F}} \oplus \hat{\mathbf{F}}^{(s)}$ is the s^{th} embeddings for multi-perspective regularization (Eq. (8)).
$\overline{\mathbf{F}}$	$\mathbf{F} = \dot{\mathbf{F}} \oplus \hat{\mathbf{F}}$ is the final concatenated embeddings.
$\mathbf{P}_{ij}^{(k)}$	k^{th} path between node i and node j . Each row in \mathbf{P} is drawn from $\tilde{\mathbf{F}}$.
\mathbf{W}	The path attention matrix computed by LSTM (Section 3.2.2).
\mathbf{Z}	The final predictions from classifier ($f_{mlp}(\cdot)$).
θ_1	The trainable parameters in encoder $f_{enc}(\cdot)$.
θ_2	The trainable parameters in LSTM ($f_{lstm}(\cdot)$).
θ_3	The trainable parameters in classifier ($f_{mlp}(\cdot)$).
\mathcal{L}_{sup}	The supervised loss computed from Eq. (6).
\mathcal{L}_{unsup}	The unsupervised loss consisted of \mathcal{L}_{con} and \mathcal{L}_{tri} (Eq. (5)).
\mathcal{L}_{con}	The consistency loss for multi-perspective regularization computed from Eq. (8).
\mathcal{L}_{tri}	The triplet loss for semantic enhancing computed from Eq. (10).

path. A second research direction for semi-supervised learning on graphs is to design powerful regularization methods for regularizing GNNs [8, 21, 27, 33]. For example, UGNN [27] utilized the unlabeled data by constructing them as subgraphs; GraphMix [39] introduced the mixup strategy [45] in GNNs by utilizing linear interpolation between two nodes for data augmentation; GRAND [8] used the DropNode method (which is similar to DropEdge [33]) to perturb the graph structure for data augmentation. Another branch of methods focuses on contrastive learning [15, 36, 38, 47], proposing contrastive loss for optimizing among multiple views. For example, Sun et al. [36], Veličković et al. [38] and Hassani and Khasahmadi [15] tried to fuse the global graph information and local graph information by proposing different contrastive losses; Zhou et al. [47] injected label information in the contrastive learning process. These contrastive learning methods generally encouraged the embeddings to obtain more neglected information.

In contrast, CustomGNN approach integrates the multi-view concept from contrastive learning and incorporates the regularization idea, with a specific focus on semantics, aiming to enhance consensus among semantic representations. Specifically, we perform random walks to generate various subgraphs in each iteration. Each of these subgraphs could represent a distinct view of the whole graph and each of the corresponding embeddings contains a distinct semantic. After multiple iterations, we get multi-perspective views and semantics. Finally, we compute the consistency loss among them to augment the consensus of multi-perspective semantics.

3. The Proposed Method

The overall architecture of CustomGNN is illustrated in Figure 2. Given a graph G with encoded features, we develop a path re-weighting module (blue stream) to capture the customized high-level semantic information, and a multi-hop GNN module (orange stream) to capture the generic graph information. The most salient part proposed in CustomGNN is to re-weight each sub-path by an LSTM-based neural network model, which customizes the paths' importance for a specific downstream task. Table 1 provides the definitions of the notations we used in this paper.

3.1. Feature Encoder

Let n and d represent the number of nodes and feature dimension respectively. In the beginning, a feature encoder f_{enc} is employed to compress the sparse features $\mathbf{F} \in \mathbb{R}^{n \times d}$ into low dimensional dense features $\{\tilde{\mathbf{F}} = f_{enc}(\mathbf{F}; \theta_1) \mid \tilde{\mathbf{F}} \in \mathbb{R}^{n \times D}\}$, where D denotes the dimension of encoded features. The encoder $f_{enc}(\cdot)$ is implemented as: $f_{enc}(\mathbf{F}; \theta_1) = \mathbf{F}\theta_1$, where $\theta_1 \in \mathbb{R}^{d \times D}$ are the trainable parameters in $f_{enc}(\cdot)$.

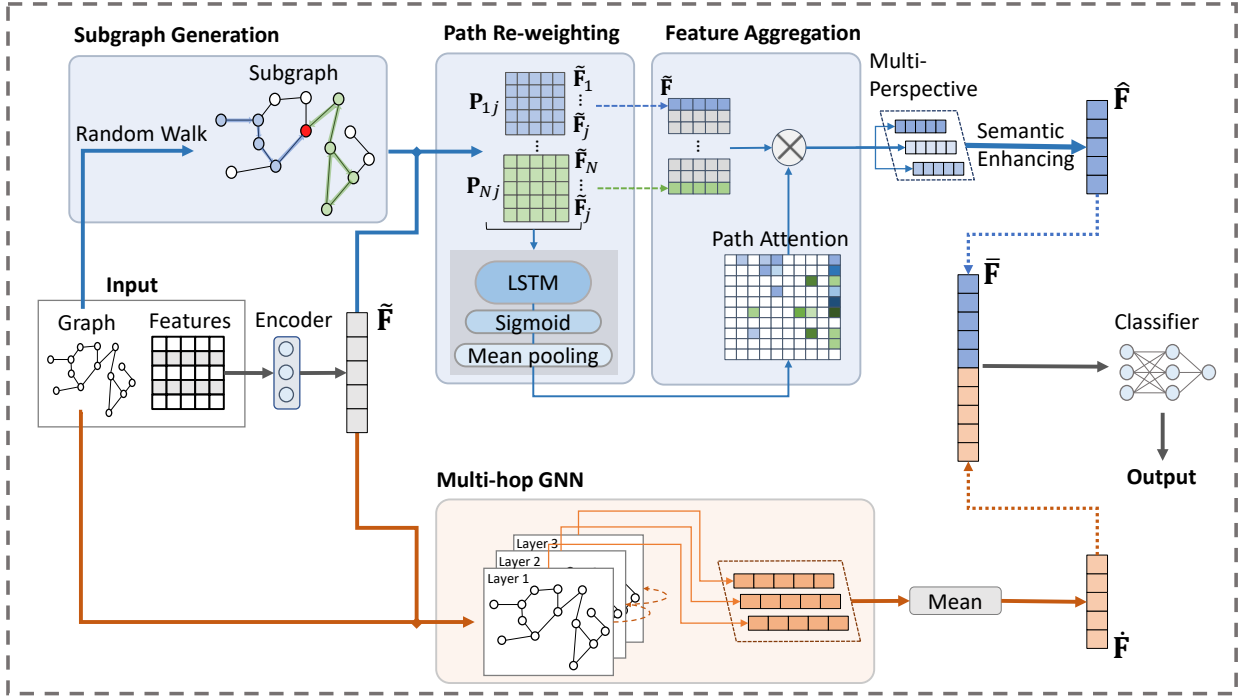


Figure 2: The overall architectural diagram of CustomGNN. Here, \otimes denotes matrix multiplication operation. There are two paths in CustomGNN. The first path highlighted in blue uses random walk to generate sub-paths (a subgraph), then, the path re-weighting module is utilized in these sub-paths for generating customized feature $\hat{\mathbf{F}}$. The orange line indicates that we utilize a simple multi-hop GNN to generate general feature $\tilde{\mathbf{F}}$. Finally, we feed the aggregated feature $\{\tilde{\mathbf{F}} \mid \bar{\mathbf{F}} = \hat{\mathbf{F}} \oplus \tilde{\mathbf{F}}\}$ into classifier to obtain the predictions.

3.2. LSTM-Based Path Re-Weighting

3.2.1. Subgraph Generation

A random walk on the graph could generate multiple paths and extract corresponding node pairs. For example, setting the window size to three and path length to four, we can get a path (x_1, x_2, x_3, x_4) and a set of sub-paths, i.e., (x_1, x_2) , (x_2, x_3) , (x_3, x_4) , (x_1, x_2, x_3) , (x_2, x_3, x_4) . The starting and ending node in each sub-path construct a node pair. As illustrated in Figure 2, we perform multiple random walks from a single point, which will generate multiple paths with the same starting node. These paths with the same starting node can be regarded as a subgraph. Therefore, a subgraph can be generated by multiple random walks.

3.2.2. Path Re-Weighting

In traditional GNNs such as GCN [23], GCNII [6], SGC [41] and S²GC [49], paths were equally treated in their loss functions. Some other methods, such as GAT [37], have computed the attention between a node pair. However, this attention is computed mainly according to the similarity of the node features, and the *specific high-level semantic information* (such as the importance of paths between this pair of nodes) has been lost. Therefore, attention learned in this manner may not always be optimal for a given downstream task. To better understand the importance of path re-weighting, we take the Wikipedia knowledge graph as an example. Each path in the graph reflects a piece of knowledge in a particular domain. If we want to enhance the performance of medical Q&A by exploiting Wikipedia knowledge graph, some general knowledge that is not related to the medical domain should be de-emphasized. Thus, we re-weight the paths to indicate their importance scores so that the crucial knowledge for a specific task can be selected.

In the path re-weighting step, we generate path weight w_{ij} for a node pair (x_i, x_j) . On account of homophily assumption [28], nodes with the same label are more likely to be appeared in a same subgraph, so a subgraph must imply some semantic information about the labels. Therefore, the challenge is how to extract the implicit high-level

semantics from subgraphs (paths). Naturally, we can use a sequence model (e.g., LSTM [19]) to extract the high-level semantic information from paths.

Formally, if we have a node pair (x_i, x_j) and paths from x_i to x_j , i.e., $\mathbf{P}_{ij}^{(0)}, \dots, \mathbf{P}_{ij}^{(k)}, \dots, \mathbf{P}_{ij}^{(N-1)}$, the path weight w_{ij} can be computed by the followed formulation:

$$w_{ij} = \frac{1}{N} \sum_{k=0}^{N-1} S(f_{lstm}(\mathbf{P}_{ij}^{(k)}; \theta_2)), \quad (1)$$

where f_{lstm} and θ_2 denote the LSTM model and the trainable parameters in LSTM respectively. $S(\cdot)$ represents Sigmoid activation function. The path matrix $\mathbf{P}_{ij} \in \mathbb{R}^{L \times D \times N}$ is the feature representation of sampled path sequences, where L , D and N represent the path length, dimension of $\tilde{\mathbf{F}}$, and the number of paths between node pair (x_i, x_j) .

3.3. Semantic Aggregation

3.3.1. Re-Weighted Attention

We aggregate the semantic information from re-weighted paths in an attention matrix. Concretely, the path weights $\{w_{ij} | 0 \leq i, j < n\}$ are used to construct path attention matrix $\mathbf{W} \in \mathbb{R}^{n \times n}$ whose role is similar to the attention matrix in GAT or the Laplacian matrix in GCN. Each weight value w_{ij} is an entry of \mathbf{W} .

3.3.2. Feature Aggregation

In this step, we conduct a convolution operation on \mathbf{W} to embed features $\tilde{\mathbf{F}}$. This operation could aggregate the high-level semantic information of a subgraph to center node (j^{th} node) of this subgraph. The aggregating operation can be expressed as follow:

$$\hat{\mathbf{F}}_j = \sum_{i=0}^{n-1} w_{ij} \cdot \tilde{\mathbf{F}}_{ij}, \quad (2)$$

where w_{ij} is the attention (weight) value of i^{th} node to j^{th} node, n represents the number of nodes, and $\hat{\mathbf{F}}_j$ denotes the node embedding of j^{th} node.

3.4. Infusion with Multi-Hop GNN

3.4.1. Multi-Hop GNN

To prevent some graph-structured information from being lost, the multi-hop GNN module is used to learn the generic graph information. In this module, we compute the means of all graph convolutional layers' output $\tilde{\mathbf{F}}$. Formally, $\hat{\mathbf{F}}$ is computed as follow:

$$\hat{\mathbf{F}} = \frac{1}{H+1} \sum_{h=0}^H \mathbf{A}^h \tilde{\mathbf{F}}, \quad (3)$$

where H is a hyperparameter that denotes the number of graph convolutional layers.

3.4.2. Semantic Infusion

Finally, we infuse the *high-level semantic information* into generic graph information by concatenating $\hat{\mathbf{F}}$ and $\tilde{\mathbf{F}}$, and feed them into an multi-layer perceptron (MLP) followed by a softmax function $\sigma(\cdot)$ to get the prediction \mathbf{Z} . The equation can be written as $\mathbf{Z} = \sigma(f_{mlp}(\hat{\mathbf{F}} \oplus \tilde{\mathbf{F}}; \theta_3))$, where θ_3 is the trainable parameters in $f_{mlp}(\cdot)$, and \oplus represents the concatenating operation.

3.5. Loss Function and Joint Training

In semi-supervised learning problem, the majority of training samples are unlabeled, so how to leverage these unlabeled data is important. Firstly, in the subgraph generation process (Section 3.2.1), we randomly sample some subgraphs each iteration, these subgraphs can be seen as a new perspective of our data. Then, we propose multi-perspective regularization for regularizing these perspectives. Secondly, in order to enhance the distinctiveness among the generated path semantics, we first employ path re-weighting module to extract the semantic of each paths, and then, we minimize the distance of same semantics and maximize the distance of different one via triplet loss function. Therefore, the unsupervised loss consists of the two parts. Algorithm 1 illustrates the whole training and predicting process. Next, we will introduce the training process in detail.

3.5.1. Overall Loss Function

As formulated in Eq. (4), our loss function contains supervised and unsupervised loss, and we use λ to control the trade-off between them:

$$\mathcal{L} = \mathcal{L}_{sup} + \lambda \mathcal{L}_{unsup}. \quad (4)$$

The unsupervised loss is a combination of the triplet loss (Eq. (10)) and consistency loss (Eq. (8)) showed in Eq. (5), and we use two hyper-parameters λ_1 and λ_2 to control the balance of the two parts:

$$\mathcal{L}_{unsup} = \lambda_1 \mathcal{L}_{con} + \lambda_2 \mathcal{L}_{tri}. \quad (5)$$

With labeled data \mathbf{Y}^L and the predictions $\mathbf{Z}^{(s),L}$ from MLP, we compute the average cross entropy loss of $\{\mathbf{Z}^{(s),L} | 1 \leq s \leq S\}$:

$$\mathcal{L}_{sup} = -\frac{1}{S} \sum_{s=1}^S [\mathbf{Y}^L \log \mathbf{Z}^{(s),L} + (1 - \mathbf{Y}^L) \log (1 - \mathbf{Z}^{(s),L})]. \quad (6)$$

Algorithm 1 CustomGNN

Input: adjacency matrix \mathbf{A} , feature matrix \mathbf{F} , training labels \mathbf{Y}^L ;

Hyperparameters: loss trade-off parameters λ , λ_1 and λ_2 , learning rate η , GNN propagation step H , the number of perspectives for regularization S ;

Parameters: encoder $f_{enc}(\mathbf{F}; \theta_1)$, sequence model (LSTM) $f_{lstm}(\mathbf{P}; \theta_2)$, classifier $f_{mlp}(\bar{\mathbf{F}}; \theta_3)$.

Output: predictions \mathbf{Z} .

```

1: while not converged do
2:   initialize  $\mathbf{W}$  with 0;
3:   for  $s=0$  to  $s < S$  do
4:     Encode input features as Section 3.1;
5:     Generate subgraphs for perspective  $s$  by random walk;
6:     Construct path attention matrix from sampled paths via Eq. (1);
7:     Aggregate subgraph information via Eq. (2);
8:     Semantic enhancing via Eq. (10);
9:     Aggregate generic graph information via Eq. (3);
10:    Semantic infusion and prediction as described in Section 3.4.2, i.e.,  $\mathbf{Z}^{(s)} = \sigma(f_{mlp}(\bar{\mathbf{F}}^{(s)}))$ ;
11:  end for
12:  Compute the unsupervised loss  $\mathcal{L}_{unsup}$  via Eq. (5);
13:  Compute the supervised loss  $\mathcal{L}_{sup}$  via Eq. (6);
14:  Update the parameters  $\theta_1$ ,  $\theta_2$  and  $\theta_3$  by gradients descending:  $\Theta = \Theta - \eta \nabla_{\Theta} (\mathcal{L}_{sup} + \lambda \mathcal{L}_{unsup})$ ;
15: end while
16: Output prediction  $\mathbf{Z}$  as described in Section 3.5.4, i.e.,  $\mathbf{Z} = \sigma(f_{mlp}(\bar{\mathbf{F}}))$ .
    
```

3.5.2. Multi-Perspective Regularization

To improve robustness and prevent over-fitting, we propose multi-perspective regularization by improving the consistency regularization [1], which encourages that different perspectives could get a consistent result. The main advantage is that the multiple perspectives are sampled from the input graph by random walk, which could capture and highlight different information so as to obtain a better regularization result.

In doing so, we generate S perspectives each epoch, each perspective is constructed by a separate path generation and re-weighting module (Section 3.2), and produce S different feature matrices $\{\hat{\mathbf{F}}^{(s)} | 1 \leq s \leq S\}$. We concatenate $\hat{\mathbf{F}}^{(s)}$ with multi-hop GNN feature $\hat{\mathbf{F}}$ to get enhanced feature $\{\bar{\mathbf{F}}^{(s)} | \bar{\mathbf{F}}^{(s)} = \hat{\mathbf{F}} \oplus \hat{\mathbf{F}}^{(s)}\}$, the enhanced features $\bar{\mathbf{F}}^{(s)}$ are then fed into the MLP module to get the predictions $\{\mathbf{Z}^{(s)} | \mathbf{Z}^{(s)} = f_{mlp}(\bar{\mathbf{F}}^{(s)})\}$. The S predictions $\{\mathbf{Z}^{(s)} | 1 \leq s \leq S\}$ produced from S perspectives are used for consistency regularization.

The purpose of this regularization is to minimize the L_2 distance among the predictions $\mathbf{Z}^{(s)}$. For example, setting $S = 2$, we aim at minimizing $\|\mathbf{Z}^{(1)} - \mathbf{Z}^{(2)}\|_2^2$. To achieve this goal, we first need to obtain the average prediction for i^{th} node, i.e., $\bar{\mathbf{Z}}_i = 1/S \sum_{s=1}^S \mathbf{Z}_i^{(s)}$. Then, we sharpen [1] the $\bar{\mathbf{Z}}_i$ with temperature T :

$$\bar{\mathbf{Z}}'_{ic} = \frac{\bar{\mathbf{Z}}_{ic}^{1/T}}{\sum_{c=0}^{C-1} \bar{\mathbf{Z}}_{ic}^{1/T}}, \quad (7)$$

where $\bar{\mathbf{Z}}'_{ic}$ is the sharpened average prediction of i^{th} node in c^{th} class. Finally, we compute the L_2 norm distance between the sharpened average prediction and S individual predictions. The consistency loss can be written as:

$$\mathcal{L}_{con} = \frac{1}{S} \sum_{s=1}^S \sum_{i=0}^{n-1} \|\mathbf{Z}_i^{(s)} - \bar{\mathbf{Z}}'_i\|_2^2. \quad (8)$$

3.5.3. Semantic Enhancing with Triplet Loss

Intuitively, the high-level semantics is implied in the labels for node classification task. Therefore, the essence of *semantic enhancing* is to make the high-level semantic of paths in same label become close and different labels become distant.

$$\mathbf{I}_{ij} = \begin{cases} 1, & \mathbf{Y}_i = \mathbf{Y}_j, \\ 0, & \mathbf{Y}_i \neq \mathbf{Y}_j. \end{cases} \quad (9)$$

The matrix $\mathbf{I} \in \{0, 1\}^{n \times n}$ is introduced to indicate whether the labels are the same or not. In Eq. (9), $\mathbf{Y} \in \{0, 1\}^{n \times C}$ denotes the one-hot label vector, C represents the number of classes. Notably, the labeled i^{th} node $\mathbf{Y}_i \in \mathbf{Y}^L$ is obtained from training set directly, and the unlabeled j^{th} node $\mathbf{Y}_j \in \mathbf{Y}^U$ is ‘‘guessed’’ by our model to get a pseudo label. The pseudo labels can be generated by $\{\mathbf{Y}_j = \text{argmax}(\mathbf{Z}_j) | \mathbf{Y}_j \in \mathbf{Y}^U\}$, where \mathbf{Z} denotes the probabilities predicted by CustomGNN. Then, the positive node pairs $(\hat{\mathbf{F}}_i^{pos}, \hat{\mathbf{F}}_j^{pos})$ and negative node pairs $(\hat{\mathbf{F}}_i^{neg}, \hat{\mathbf{F}}_j^{neg})$ can be sampled out. We use triplet loss [34] to minimize the L_2 norm distance between positive node pairs and maximize the distance between negative node pairs. The loss function is as follows:

$$\mathcal{L}_{tri} = \|\hat{\mathbf{F}}_i^{pos} - \hat{\mathbf{F}}_j^{pos}\|_2 + \text{RELU}(m - \|\hat{\mathbf{F}}_i^{neg} - \hat{\mathbf{F}}_j^{neg}\|_2), \quad (10)$$

where m is a hyperparameter that represents the margin between negative node pairs.

3.5.4. Inference

To avoid the path attention matrix \mathbf{W} being too sparse we compute this matrix S times ($S = 4$ in our setting) by S perspectives and add them together to get a new path attention matrix $\{\mathbf{W} | \mathbf{W} = \sum_{s=1}^S \mathbf{W}^{(s)}\}$. The final path attention matrix is used to compute $\hat{\mathbf{F}}$ as Eq. (2). Meanwhile, $\hat{\mathbf{F}}$ is computed by multi-hop GNN module. At last, the concatenated embedding $\bar{\mathbf{F}}$ is fed into classifier, i.e., $f_{mlp}(\cdot)$ to get the final prediction \mathbf{Z} .

3.6. Complexity Analysis

CustomGNN consists of four main components: subgraph generation, path re-weighting, feature aggregation, and multi-hop GNN. To analyze the time complexity of the model, we need to consider the time complexity of each component and sum them up.

- Subgraph generation: this component uses random walk to generate subgraphs from the original graph. Assume n is the number of nodes, k is the iterations of random walk, so the time complexity of this component is $O(kn)$.
- Path re-weighting: this component uses a LSTM-based path weighting strategy to calculate multiple path attention maps from the subgraphs. Assume l is the average length of each path, and h is the hidden size of LSTM, so for average p paths in each subgraph, the time complexity of this component is $O(plh^2)$. Notably, LSTM can be replaced by other more efficient sequence models, e.g., GRU (Gate Recurrent Unit) and self-attention neural networks.

Table 2

Details of datasets after preprocessing.

Dataset	Nodes	Edges	Classes	Features	Label Rate
Cora	2,708	5,429	7	1,433	0.0516
Citeseer	3,327	4,732	6	3,703	0.0360
PubMed	19,717	44,338	3	500	0.0030
Cora-Full	19,749	63,262	68	8,710	0.0689
Coauthor CS	18,333	81,894	15	6,805	0.0164
Amazon Computer	13,752	245,861	10	767	0.0145
Amazon Photo	7,650	119,081	8	745	0.0209

- Feature aggregation: this component uses a weighted sum operation to aggregate features through the path attention maps. The time complexity of this component is $O(nd)$, where d is the dimension of node features.
- Multi-hop GNN: this component uses a standard multi-hop GNN to infuse the general structural information. The time complexity of this component is $O(onmd)$, where o is the number of hops or layers, and m is the average degree of nodes in the original graph.

Overall, the training time complexity of CustomGNN is $O(kn + plh^2 + nd + onmd)$. In the inference phase, the path attention map is directly loaded from saved parameters. Therefore, inference time complexity is $O(nd + onmd)$, which is approximately the same as other popular GNNs.

4. Experiments

4.1. Datasets

Following the community convention, we use three benchmark graphs, i.e., Cora, Citeseer and PubMed with their standard public splits in Planetoid [44], which contains 20 nodes per class for training and 1000 nodes for testing. We also did experiments on four publicly available large datasets, i.e., Cora Full, Coauthor CS, Amazon Photo, and Amazon Computers with their experimental settings in Shchur et al. [35].

These datasets can be downloaded from PyTorch-Geometric library¹. The datasets details are shown in Table 2. Label rate is the fraction of nodes in training set (the number of training nodes is 20 per class) that can be computed as $(\#class \cdot 20) / \#node$.

4.2. Baselines

For the three standard split datasets, we choose 20 GNN SOTAs for comparison, including GCN [23] and its evolutions [6, 41, 49], deep GNNs like MixHop [45] and APPNP [24], and five augmentation-based GNNs [8, 33, 39, 43]. For the other four larger datasets, we choose baseline methods that can be scaled to large graphs, including a two-layer MLP (input layer \rightarrow hidden layer \rightarrow output layer) with 128-hidden units, standard GCN and GAT, and two regularization based methods, i.e., GRAND [8] (using MLP as the backbone) and P-reg [43] (using GCN as the backbone).

4.3. Overall Results

Table 3 compares the accuracy of CustomGNN with 21 SOTA methods. The results of these methods are taken from their original papers directly. It shows that CustomGNN achieves the SOTA accuracy on all three standard datasets, i.e., Cora, Citeseer, and PubMed. It is notable that CustomGNN shows impressive improvements on Citeseer, which may be because the citation graph on Citeseer implies more semantics, and CustomGNN has effectively extracted and utilized this semantic information. We will further analyze this finding in Section 4.5.

Table 4 compares the accuracy of CustomGNN with three traditional baselines and two regularization based GNNs. The experiments strictly follow the evaluation protocol of Shchur et al. [35]. The results of the MLP, GCN, GAT, GRAND and CustomGNN are averaged over 100 runs on different random seed for train/test set split and

¹<https://pytorch-geometric.readthedocs.io>

Table 3

Results on 3 standard split datasets with over 100 runs. Some papers do not report their std values, which are marked by “*”. **Bold** denotes the best performance, underline denotes the second best.

Method	Cora	Citeseer	PubMed
GCN (2017)	81.5± *	70.3± *	79.0± *
GraphSAGE (2017)	78.9±0.8	67.4±0.7	77.8±0.6
FastGCN (2018)	81.4±0.5	68.8±0.9	77.6±0.5
GAT (2018)	83.0±0.7	72.5±0.7	79.0±0.3
MixHop (2018)	81.9±0.4	71.4±0.8	80.8±0.6
APPNP (2019)	83.8±0.3	71.6±0.5	79.7±0.3
DropEdge (2020)	82.8± *	72.3± *	79.6± *
SGC (2019)	81.0±0.0	71.9±0.1	78.0±0.0
GMNN (2019)	83.7± *	72.9± *	81.8± *
GraphNAS (2019)	84.2±1.0	73.1±0.9	79.6±0.4
GCNII (2020b)	85.5±0.5	73.4±0.6	80.2±0.4
GRAND (2020)	<u>85.4±0.4</u>	<u>75.4±0.4</u>	<u>82.7±0.6</u>
GraphMix (2021)	<u>83.9±0.6</u>	<u>74.5±0.6</u>	<u>81.0±0.6</u>
P-reg (2021)	82.8±1.2	71.6±2.2	77.4±1.5
superGAT (2021)	84.3±0.6	72.6±0.8	81.7±0.5
S ² GC (2021)	83.5±0.0	73.6±0.1	80.2±0.0
GraphSAD (2021)	83.0±0.4	71.2±0.2	79.6±0.1
CGNN (2022)	82.5±0.6	72.1±0.7	78.9±0.5
CustomGNN	85.5±0.2	76.0±0.4	83.3±0.2

Table 4

Results on 4 large datasets with over 100 runs on different random seed for train/test set split and different random seed for weight initialization. **Bold** denotes the best performance, underline denotes the second best and “-” denotes the original authors does not run this experiment.

Method	Cora-Full	Coauthor CS	Amazon Computer	Amazon Photo
MLP	18.3±4.9	88.3±0.7	57.8±7.0	73.5±9.7
GCN (2017)	9.0±4.9	88.1±2.7	42.3±16.0	61.4±12.3
GAT (2018)	13.7±5.2	90.3±1.4	65.4±15.3	80.8±9.5
GRAND (2020)	<u>42.3±6.5</u>	<u>92.9±0.5</u>	80.1±7.2	72.9±2.1
P-reg (2021)	-	<u>92.6±0.3</u>	<u>81.7±1.4</u>	<u>91.2±0.8</u>
CustomGNN	44.2±1.2	93.4±0.3	81.9±0.8	92.0±3.4

different random seed for weight initialization. The results of P-reg are taken from its original paper. It shows that CustomGNN outperforms the other five methods on all four large datasets.

4.4. Ablation Study

Table 5 illustrates the results of ablation study. This study evaluates the contributions of different components in CustomGNN.

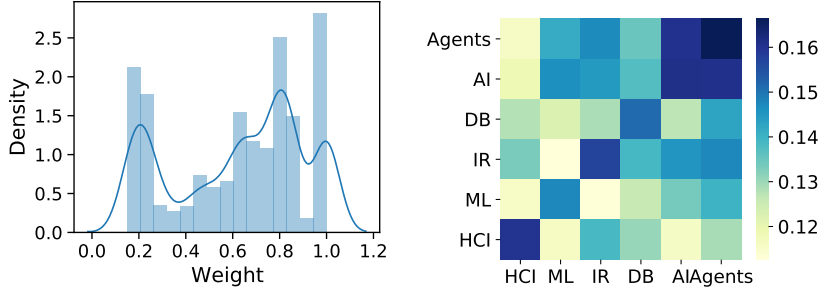
Without Path Re-Weighting. In this part, we only use the multi-hop GNN module to generate node embeddings, i.e., $\bar{\mathbf{F}} = \hat{\mathbf{F}}$, the path re-weighting module containing unsupervised loss (Eq. (5)) is removed. So the learned embedding only contains generic graph information. This result can be regarded as a baseline.

Without Multi-Hop GNN. This ablation experiment only uses the path re-weighting module to generate the final node embeddings, i.e., $\bar{\mathbf{F}} = \hat{\mathbf{F}}$. In addition, to get a dense path attention matrix (\mathbf{W}), we sample paths for all nodes, i.e.,

Table 5

Ablation studies. The accuracy of CustomGNN without specific component. The number in parentheses is the decay of accuracy after removing this component.

Component	Cora	Citeseer	PubMed
w/o path re-weighting	79.2(-6.3)	68.7(-7.3)	77.8(-5.5)
w/o multi-hop GNN	83.4(-1.2)	75.4(-0.6)	81.6(-1.7)
w/o semantic enhancing	84.6(-1.2)	75.2(-0.8)	81.6(-1.7)
w/o multi-perspective	84.2(-1.3)	75.3(-0.7)	79.2(-4.1)
original	85.5	76.0	83.3



(a) Distribution of re-weighted path attentions. (b) Visualization of relevances among categories.

Figure 3: (a) The visualization of re-weighted path attentions on Citeseer. We filter out some noisy points whose weight is less than 0.15. (b) The visualization of relevance between different categories on Citeseer. The weight on (i, j) means how much the i^{th} category is influenced by j^{th} category.

fixing sampling batch size to $\#nodes/S$. It is obvious that the classification results are better than w/o path re-weighting, indicating that the path re-weighting module learns more effective information than generic graph information learned by multi-hop GNN.

Without Semantic Enhancing. The unsupervised loss is only computed by consistency regularization loss to show the efficacy of the proposed semantic enhancing method with triplet loss. The results indicate that the accuracy exhibits a slight decline when the semantic enhancing regularization term is omitted.

Without Multi-Perspective Regularization. The unsupervised loss is only computed by triplet loss to show the efficacy of the proposed multi-perspective regularization. To this end, we first set $S = 1$ for using only one perspective. Second, we sample paths for all nodes to ensure that this perspective can get more complete information. Third, because there is no consistency regularization, we decrease the dropout rate to avoid overfitting. The results show that the exclusion of the multi-perspective regularization term evidently leads to a decline in the results, particularly when dealing with relatively larger datasets, i.e., PubMed.

4.5. Analysis

The re-weighted attentions learned by CustomGNN are customized for different downstream tasks. For example, Figure 3(a) shows the distribution of re-weighted attentions for Citeseer node classification task, which is quite diverse. To better understand these attentions and how CustomGNN benefits the results, we provide some semantic analyses. After that, we study three metrics of our performance, i.e., generalization, robustness, and over-smoothing. In our experiments, we compared CustomGNN with two traditional GNNs (GCN [23] and GAT [37]) and a GNN SOTA (GRAND [8]) which concentrates on resolving the three issues.

4.5.1. Semantics Explanation

In order to mine the semantics of re-weighted paths, we use Citeseer as an example. Papers on Citeseer are classified into 6 categories as described in Table 6. Based on this dataset, the task is to classify a given paper to its

Table 6

Summary of paper citation graph on Citeseer.

Category	Number
Agents	239
Artificial Intelligence (AI)	537
Data Base (DB)	619
Information Retrieval (IR)	633
Machine Learning (ML)	560
Human-Computer Interaction (HCI)	463

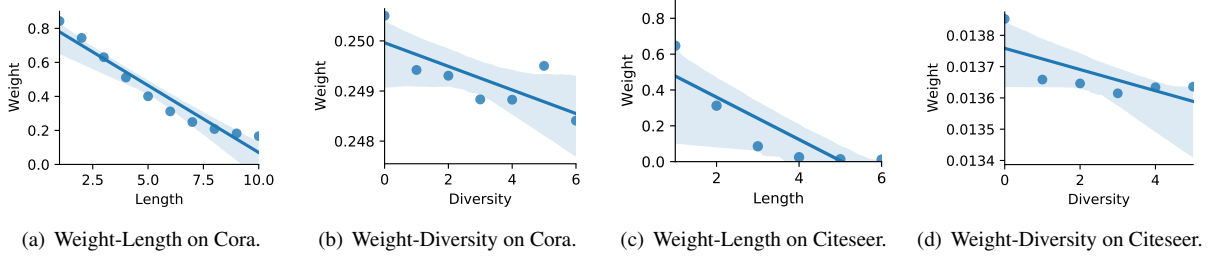


Figure 4: (a), (b) and (c), (d) are the mean correlations between weight and two properties (length and diversity) of paths on Cora and Citeseer respectively. In (b) and (d), to remove the influence of length, the path length is fixed on 10. Y-axis denotes the average weight of the corresponding paths.

category. After training the model, we generate multiple paths for a pair of nodes, the average of these paths' weights is the average relevance weight between the corresponding categories of this pair of nodes. We visualize the relevance weights among different categories in Figure 3(b).

Figure 3(b) implies a lot of information. Consistent with our intuition, the average weights of self-loop (computed from paths where the starting and ending nodes are from the same category) is the largest, e.g., the weight of (IR, IR) is larger than $(IR, others)$. Moreover, from Figure 3(b), we can see that AI and $Agents$ are highly relevant with each other; AI is much influenced by ML , whereas ML is less influenced by AI ; DB influences others more than it is influenced by others, as the column of DB has smaller average weights than its corresponding line in the visualized matrix. All these results coincide with human intuitions.

4.5.2. Weight Correlation

To analyze how the properties of paths influence weight scores, we draw the correlations between weight scores and two properties of paths, i.e., length and diversity, on Figure 4. Length is defined as the number of nodes in a path; Diversity is defined as the number of different categories of labeled node in a path. For example, we have a path (x_1, x_2, x_3) and their corresponding categories $(AI, Agents, AI)$, the length and diversity of this path is three and two respectively. As demonstrated in Figures 4(a) and 4(c), correlations between two nodes decay as the distance between them becomes larger, this corresponds with the homophily assumption [28] that the correlation is strong if two nodes are adjacent; In Figures 4(b) and 4(d), the path weight increases with the reduction of node diversity. Intuitively, if a path contains fewer categories, the path contains more information and less noise about the corresponding class. This nature is helpful for the task of node classification.

4.5.3. Generalization Analysis

We examine the generalization of CustomGNN and how the path re-weighting module contributes to the generalization. To measure this, we compute the gap of cross-entropy losses between train set and validation set. The smaller gap illustrates the better generalization ability of the model. Figure 5 reports the results, and proves that the techniques of path re-weighting module in CustomGNN can prevent overfitting.

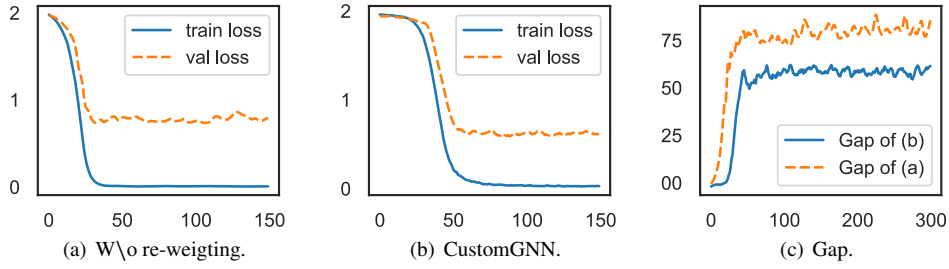


Figure 5: (a) is the loss of CustomGNN without path re-weighting, and (b) is the loss of CustomGNN. X-axis denotes training epochs, Y-axis denotes loss values. (c) illustrates the gap between train loss and validation loss of (a) and (b), Y-axis denotes the gap value.

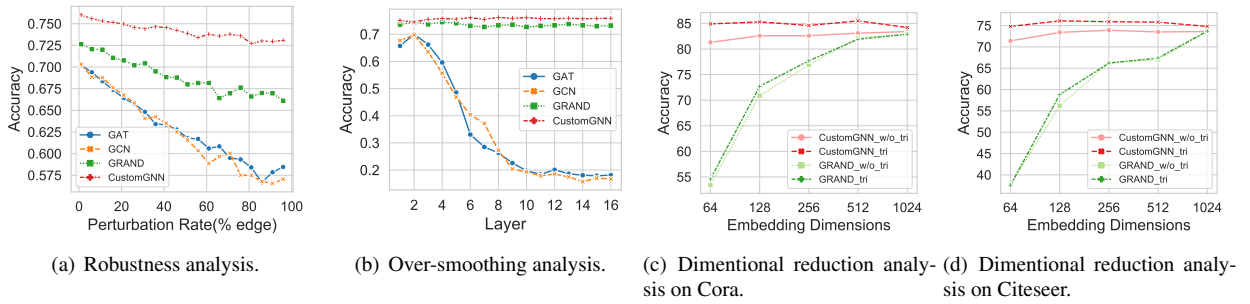


Figure 6: (a) On Robustness analysis, we gradually increase the perturbation rate (from 1% to 100%). (b) On over-smoothing analysis, for GAT, GCN, and GRAND, we increase the propagation layers; For CustomGNN, we increase the propagation layers of multi-hop GNN module, and increase the aggregation orders (window size) of the path re-weighting module meanwhile. (c) and (d) are dimensional reduction analysis, where we generally increase the embedding dimensions from 64 to 1024.

4.5.4. Robustness Analysis

We made a noise identification ability and robust analysis of CustomGNN by randomly adding a certain proportion of fake edges. In Figure 6(a), we can observe that the classification accuracy of nodes in GCN and GAT declines rapidly with the increase of fake edges. Although both CustomGNN and GRAND can maintain a slower decline rate in classification accuracy as the number of fake edges increases, CustomGNN is always superior to GRAND in robustness, and the decline curve is smoother.

4.5.5. Over-Smoothing Analysis

Lots of GNN models suffer from the over-smoothing problem. As reported in previous works [49, 2], with the increase of layer numbers, the identification of nodes in different classes becomes undistinguished, because the multiple propagation steps lead to over-mixing of information and noises [2], then, the node embeddings become similar. Figure 6(b) proved the ability of our model to relieve over-smoothing.

4.6. Dimensional Reduction Analysis

In reality, many nodes attach some auxiliary information, for example, each node on Cora-Full attaches a feature with 8710-dimension. Therefore, the high dimensional features expect low dimensional representations. In this experiment, we conduct encoder f_{enc} to reduce the feature dimension in the beginning, then, CustomGNN is compared with GRAND in different dimensions. As shown in Figures 6(c) and 6(d), with the decrease of dimension, the accuracy of GRAND declining, by contrast, the accuracy of CustomGNN is stable. The result demonstrates that CustomGNN is not sensitive to different embedding dimensions. A possible reason is that CustomGNN can extract the task-relevant information more efficiently. Alternatively, from Figures 6(c) and 6(d), it is notable that the triplet loss which is used

for semantic enhancing can benefit more to CustomGNN than GRAND. This might be that the CustomGNN captures more semantic information that has the chance to be enhanced by the proposed triplet loss.

5. Conclusions

In this work, we study graph neural networks (GNN) from a new view, i.e., customizing GNN for a specific downstream task, and present a new GNN framework, namely, Customized Graph Neural Network with Path Reweighting (CustomGNN). CustomGNN can resolve the inherent issues of traditional GNNs, i.e., over-smoothing, over-fitting, and non-robustness to data attack. In CustomGNN, we capture customized semantic information from weighted paths, which is then infused with the generic graph information extracted from multi-hop GNN module. Moreover, based on the well-designed framework, we generate multi-perspective subgraphs to regularize the extracted semantics, and enhance the semantics by proposing a triplet loss with pseudo-labels. Extensive experiments show that CustomGNN outperforms most SOTAs. In addition, we analyze the semantics learned by CustomGNN and demonstrate the superiority of CustomGNN in terms of resistance to over-smoothing and robustness to data attack. In future work, we aim to apply the impressive semantic extraction ability of CustomGNN to more graph-based tasks.

CRedit authorship contribution statement

Jianpeng Chen: Conceptualization, Methodology, Software, Visualization, Investigation, Writing - Original Draft, Writing - Review & Editing. **Yujing Wang:** Conceptualization, Methodology, Formal analysis, Writing - Original Draft, Writing - Review & Editing. **Ming Zeng:** Conceptualization, Methodology, Formal analysis, Writing - Review & Editing. **Zongyi Xiang:** Validation, Visualization, Writing - Original Draft. **Bitan Hou:** Conceptualization. **Yunhai Tong:** Writing - Review & Editing. **Ole Mengshoel:** Writing - Review & Editing. **Yazhou Ren:** Supervision, Project administration, Funding acquisition, Writing - Review & Editing.

Declaration of Competing Interest

The authors declare that they have no known competing financial interests or personal relationships that could have appeared to influence the work reported in this paper.

Acknowledgements

This work was supported in part by National Key Research and Development Program of China (No. 2020YFB2103402), Shenzhen Science and Technology Program (No. JCYJ20230807115959041), and the open project of Sichuan Provincial Key Laboratory of Philosophy and Social Science for Language Intelligence in Special Education (No. YYZN-2023-3).

A. Reproducibility

A.1. Implementation Details

We use PyTorch to implement CustomGNN and all of its components. The LSTM we used in path re-weighting module is implemented in the package of torch.nn.LSTM. For the results of large datasets we reported (in Table 4), the implementation of GRAND comes from its public source code², the implementations of GCN and GAT layer come from the PyTorch-Geometric library, and the results of P-reg are taken from its original paper directly. We adopt Adam to optimize the parameters of all models in our paper, and we perform early stopping strategy to control the training epochs. We employ Dropout in the adjacency matrix, path-weight matrix, encoder, and each layer of prediction module (i.e., MLP) as a generally used trick for preventing overfitting. The experiments of Cora, Citeseer are conducted on a Tesla V100 with 80GB memory size, the experiments of PubMed, Cora Full, Amazon Computer, Amazon Photo and Cauthor CS are conducted on Tesla V100 with 32GB memory size. As for the software version, we use Python 3.8.5, PyTorch 1.7.1, NumPy 1.19.2, and CUDA 11.0.

²<https://github.com/Grand20/grand>

Table 7

Hyperparameters of CustomGNN for reproducing the results reported in Table 3.

Hyperparameters	Cora	Citeseer	PubMed
Learning rate η	0.01	0.01	0.1
Dropout rate of MLP layers	0.5	0.5	0.8
Dropout rate of encoder	0.6	0.6	0.5
Dropout rate of Path Weight Adjacency matrix	0.6	0.6	0.6
Dropout rate of Adjacency matrix	0.5	0.5	0.5
LSTM hidden units	128	128	128
Early stop epochs	300	200	100
L2 weight decay rate	5e-4	5e-4	5e-4
Triplet loss coefficient λ_1 in Eq. (5)	1.0	1.0	1.0
Consistency loss coefficient in Eq. (5)	1.0	1.0	1.0
Tradeoff λ , $\hat{F} \oplus \lambda \hat{F}$	1.0	10.0	1.0
Embedding dimension (output dimension of Encoder)	512	512	256
Batch size of path sampling	300	300	500
Path length of path sampling	12	10	6
Window size of path sampling	8	5	5
Orders/Layers of Multi-hop GNN module	8	4	5
Number of negative sampling for triplet loss	5000	10000	5000
Number of positive sampling for triplet loss	15000	10000	5000
Margin of negative samples for triplet loss	0.1	1	1
Temperature of consistency loss T	0.5	0.5	0.2
Regularization times S	4	4	4

A.2. Hyperparameter Details

We show the hyperparameters of CustomGNN for results in Table 3. These hyperparameters can be divided into 4 groups, the first controls the training process which is shown in 1 to 12 rows of Table 7, the second controls the customized attention module which is shown in 13 to 16 rows of Table 7, the third controls the triplet loss which are shown in 17 to 20 rows of Table 7, and the fourth control the the consistency loss which are shown in 21 to 22 rows of Table 7.

References

- [1] Berthelot, D., Carlini, N., Goodfellow, I., Papernot, N., Oliver, A., Raffel, C., 2019. Mixmatch: A holistic approach to semi-supervised learning, in: NIPS, pp. 5050–5060.
- [2] Chen, D., Lin, Y., Li, W., Li, P., Zhou, J., Sun, X., 2020a. Measuring and relieving the over-smoothing problem for graph neural networks from the topological view, in: AAAI, pp. 3438–3445.
- [3] Chen, J., Ling, Y., Xu, J., Ren, Y., Huang, S., Pu, X., Hao, Z., Yu, P.S., He, L., 2022. Variational graph generator for multi-view graph clustering. arXiv preprint arXiv:2210.07011 .
- [4] Chen, J., Ma, T., Xiao, C., 2018. Fastgcn: Fast learning with graph convolutional networks via importance sampling, in: ICLR.
- [5] Chen, J., Yang, Z., Pu, J., Ren, Y., Pu, X., Gao, L., He, L., 2023. Shared-attribute multi-graph clustering with global self-attention, in: International Conference on Neural Information Processing, Part I (ICONIP), pp. 51–63.
- [6] Chen, M., Wei, Z., Huang, Z., Ding, B., Li, Y., 2020b. Simple and deep graph convolutional networks, in: ICML, pp. 1725–1735.
- [7] Ding, M., Tang, J., Zhang, J., 2018. Semi-supervised learning on graphs with generative adversarial nets, in: CIKM, pp. 913–922.
- [8] Feng, W., Zhang, J., Dong, Y., Han, Y., Luan, H., Xu, Q., Yang, Q., Kharlamov, E., Tang, J., 2020. Graph random neural networks for semi-supervised learning on graphs, in: NeurIPS.
- [9] Gao, Y., Yang, H., Zhang, P., Zhou, C., Hu, Y., 2019. Graphnas: Graph neural architecture search with reinforcement learning. CoRR abs/1904.09981.
- [10] Geng, X., He, X., Xu, L., Yu, J., 2022. Graph correlated attention recurrent neural network for multivariate time series forecasting. Information Sciences 606, 126–142.
- [11] Gilmer, J., Schoenholz, S.S., Riley, P.F., Vinyals, O., Dahl, G.E., 2017. Neural message passing for quantum chemistry, in: ICML, pp. 1263–1272.
- [12] Grover, A., Leskovec, J., 2016. node2vec: Scalable feature learning for networks, in: KDD, pp. 855–864.
- [13] Hamilton, W.L., Ying, Z., Leskovec, J., 2017. Inductive representation learning on large graphs, in: NIPS, pp. 1024–1034.

- [14] Hao, Z., Lu, C., Huang, Z., Wang, H., Hu, Z., Liu, Q., Chen, E., Lee, C., 2020. Asgn: An active semi-supervised graph neural network for molecular property prediction, in: KDD, pp. 731–752.
- [15] Hassani, K., Khasahmadi, A.H., 2020. Contrastive multi-view representation learning on graphs, in: Proceedings of the 37th International Conference on Machine Learning, JMLR.org.
- [16] He, L., Bai, L., Yang, X., Du, H., Liang, J., 2023. High-order graph attention network. *Information Sciences* 630, 222–234. doi:<https://doi.org/10.1016/j.ins.2023.02.054>.
- [17] He, T., Ong, Y.S., Bai, L., 2021. Learning conjoint attentions for graph neural nets.
- [18] He, T., Zhou, H., Ong, Y.S., Cong, G., 2022. Not all neighbors are worth attending to: Graph selective attention networks for semi-supervised learning. *arXiv:2210.07715*.
- [19] Hochreiter, S., Schmidhuber, J., 1997. Long short-term memory. *Neural Computation* 9, 1735–1780.
- [20] Huang, F., Yi, P., Wang, J., Li, M., Peng, J., Xiong, X., 2022. A dynamical spatial-temporal graph neural network for traffic demand prediction. *Information Sciences* 594, 286–304.
- [21] Juan, X., Zhou, F., Wang, W., Jin, W., Tang, J., Wang, X., 2023. Ins-gnn: Improving graph imbalance learning with self-supervision. *Information Sciences* 637, 118935. URL: <https://www.sciencedirect.com/science/article/pii/S0020025523005042>, doi:<https://doi.org/10.1016/j.ins.2023.118935>.
- [22] Kim, D., Oh, A., 2021. How to find your friendly neighborhood: Graph attention design with self-supervision, in: ICLR.
- [23] Kipf, T.N., Welling, M., 2017. Semi-supervised classification with graph convolutional networks, in: ICLR.
- [24] Klicpera, J., Bojchevski, A., Günnemann, S., 2019. Predict then propagate: Graph neural networks meet personalized pagerank, in: ICLR.
- [25] Lee, D.H., 2013. Pseudo-label: The simple and efficient semi-supervised learning method for deep neural networks, in: ICML.
- [26] Li, H., Cao, J., Zhu, J., Liu, Y., Zhu, Q., Wu, G., 2022. Curvature graph neural network. *Information Sciences* 592, 50–66.
- [27] Luo, X., Zhao, Y., Qin, Y., Ju, W., Zhang, M., 2024. Towards semi-supervised universal graph classification. *IEEE Transactions on Knowledge and Data Engineering* 36, 416–428. doi:[10.1109/TKDE.2023.3280859](https://doi.org/10.1109/TKDE.2023.3280859).
- [28] McPherson, M., Smith-Lovin, L., Cook, J.M., 2001. Birds of a feather: Homophily in social networks. *Annual Review of Sociology* 27, 415–444.
- [29] NT, H., Maehara, T., 2019. Revisiting graph neural networks: All we have is low-pass filters. *CoRR abs/1905.09550*.
- [30] Olivier, C., Bernhard, S., Alexander, Z., 2009. Semi-supervised learning. *Journal of the Royal Statistical Society* 172, 530–530.
- [31] Oono, K., Suzuki, T., 2020. Graph neural networks exponentially lose expressive power for node classification, in: ICLR.
- [32] Qu, M., Bengio, Y., Tang, J., 2019. GMNN: graph markov neural networks, in: ICML, pp. 5241–5250.
- [33] Rong, Y., Huang, W., Xu, T., Huang, J., 2020. Dropedge: Towards deep graph convolutional networks on node classification, in: ICLR.
- [34] Schroff, F., Kalenichenko, D., Philbin, J., 2015. Facenet: A unified embedding for face recognition and clustering, in: CVPR, pp. 815–823.
- [35] Shchur, O., Mumme, M., Bojchevski, A., Günnemann, S., 2018. Pitfalls of graph neural network evaluation. *CoRR abs/1811.05868*.
- [36] Sun, F.Y., Hoffman, J., Verma, V., Tang, J., 2019. Infograph: Unsupervised and semi-supervised graph-level representation learning via mutual information maximization, in: International Conference on Learning Representations.
- [37] Veličković, P., Cucurull, G., Casanova, A., Romero, A., Liò, P., Bengio, Y., 2018. Graph attention networks, in: ICLR.
- [38] Veličković, P., Fedus, W., Hamilton, W.L., Liò, P., Bengio, Y., Hjelm, R.D., 2019. Deep graph infomax, in: International Conference on Learning Representations. URL: <https://openreview.net/forum?id=rklz9iAcKQ>.
- [39] Verma, V., Qu, M., Kawaguchi, K., Lamb, A., Bengio, Y., Kannala, J., Tang, J., 2021. Graphmix: Improved training of gnns for semi-supervised learning, in: AAAI, AAAI Press. pp. 10024–10032.
- [40] Wei, Q., Wang, J., Fu, X., Hu, J., Li, X., 2023. Aic-gnn: Adversarial information completion for graph neural networks. *Information Sciences* 626, 166–179. URL: <https://www.sciencedirect.com/science/article/pii/S0020025522016073>, doi:<https://doi.org/10.1016/j.ins.2022.12.112>.
- [41] Wu, F., Jr., A.H.S., Zhang, T., Fifty, C., Yu, T., Weinberger, K.Q., 2019. Simplifying graph convolutional networks, in: ICML, pp. 6861–6871.
- [42] Xu, M., Wang, H., Ni, B., Zhang, W., Tang, J., 2021. Graphsard: Learning graph representations with structure-attribute disentanglement, in: ICLR.
- [43] Yang, H., Ma, K., Cheng, J., 2021. Rethinking graph regularization for graph neural networks, in: AAAI, AAAI Press. pp. 4573–4581.
- [44] Yang, Z., Cohen, W.W., Salakhutdinov, R., 2016. Revisiting semi-supervised learning with graph embeddings, in: ICML, pp. 40–48.
- [45] Zhang, H., Cisse, M., Dauphin, Y.N., Lopez-Paz, D., 2018. mixup: Beyond empirical risk minimization, in: ICLR.
- [46] Zhang, K., Zhu, Y., Wang, J., Zhang, J., 2020. Adaptive structural fingerprints for graph attention networks, in: ICLR.
- [47] Zhou, H., Gong, M., Wang, S., Gao, Y., Zhao, Z., 2023. Smgcl: Semi-supervised multi-view graph contrastive learning. *Knowledge-Based Systems* 260, 110120.
- [48] Zhu, D., Zhang, Z., Cui, P., Zhu, W., 2019. Robust graph convolutional networks against adversarial attacks, in: KDD, p. 1399–1407.
- [49] Zhu, H., Koniusz, P., 2021. Simple spectral graph convolution, in: ICLR.
- [50] Zügner, D., Akbarnejad, A., Günnemann, S., 2018. Adversarial attacks on neural networks for graph data, in: KDD, p. 2847–2856.